Technical Note

"Keyhole" Method for Accelerating Imaging of Contrast Agent Uptake[1]

Joop J. van Vaals, PhD • Marijn E. Brummer, MS • W. Thomas Dixon, PhD
Hans H. Tuithof, PhD • Hans Engels, PhD • Rendon C. Nelson, MD
Brigid M. Gerety, MD • Judith L. Chezmar, MD • Jacques A. den Boer, PhD

Magnetic resonance (MR) imaging methods with good spatial and contrast resolution are often too slow to follow the uptake of contrast agents with the desired temporal resolution. Imaging can be accelerated by skipping the acquisition of data normally taken with strong phase-encoding gradients, restricting acquisition to weak-gradient data only. If the usual procedure of substituting zeros for the missing data is followed, blurring results. Substituting instead reference data taken before or well after contrast agent injection reduces this problem. Volunteer and patient images obtained by using such reference data show that imaging can be usefully accelerated severalfold. Cortical and medullary regions of interest and whole kidney regions were studied, and both gradient- and spin-echo images are shown. The method is believed to be compatible with other acceleration methods such as half-Fourier reconstruction and reading of more than one line of k space per excitation.

Index terms: Contrast enhancement • Functional studies • Gadolinium • Image processing • Kidney, MR. 81.121411, 81.121412 • Rapid imaging

JMRI 1993; 3:671–675

[1] From Philips Medical Systems, Bldg QR, Postbus 10.000, 5680 DA Best, The Netherlands (J.J.v.V., H.H.T., H.E.); Philips Magnetic Resonance Research Center, Department of Radiology, Emory University School of Medicine, Atlanta, Ga (M.E.B., W.T.D., R.C.N., B.M.G., J.L.C.); and the Medisearch Foundation, Enschede, The Netherlands (J.A.d.B.). From the 1992 SMRI annual meeting. Received September 28, 1992; revision requested November 3; revision received November 11; accepted November 20. **Address reprint requests to** J.J.v.V.

[1] SMRI, 1993

THERE IS A RAPIDLY increasing interest in functional studies that monitor the perfusion or wash-in and washout of a contrast agent such as gadopentetate dimeglumine. In many applications, dynamic studies require high time resolution or multiple sections. Echo-planar imaging (1) has been used to achieve this (2).

The contrast in an image is determined mainly by the low-frequency data acquired in lines or profiles near the center of k space. The high-frequency data from profiles more distant from the center of k space contribute edge sharpness. For this reason, increasing the speed of imaging by reducing matrix acquisition and zero-filling always yields blurred images. When large matrix reductions are used, ringing artifact may also occur. The new "keyhole" method (Fig 1) uses substantial matrix reductions; however, instead of zero-filling, it merges the low-frequency data with high-frequency data borrowed from a reference image to prevent blurring (3–9). It is an attempt to view all of k space by peeping through a small "keyhole" of data.

Using this keyhole method, we present herein gradient- and spin-echo images of a healthy volunteer and a kidney transplant patient with up to a fivefold reduction in acquisition time. This method does not require the additional hardware necessary for echo-planar imaging. To match the capabilities of a pulse sequence with the requirements of an imaging problem, the keyhole method can be used alone or, when even greater acceleration is needed, combined with other acceleration methods based on different principles. Other methods could include half-Fourier reconstruction, reading more than one line of k space per excitation, or even echo-planar imaging itself.

• MATERIALS AND METHODS

All data were collected on 1.5-T, Gyroscan S15/ACS imagers (Philips Medical Systems, Best, The Netherlands). The image matrix size was 256 in the read direction, which was along the long axis of the body. Dynamic series of identical images were started before injection of 0.1 mmol/kg gadopentetate dimeglumine (Berlex, Wayne, NJ; Schering, Berlin, Germany) and continued until after uptake of contrast agent was complete. Dynamic images (frames) taken before or minutes after contrast agent uptake were used for the high-frequency reference data. Signal averaging was not used in the usual sense because it slows imaging. However, there is no time penalty in pooling the data from several frames to improve the signal-to-noise ratio of the reference data.

Two types of experiments were done. First, a patient with a kidney transplanted into the pelvis was examined during gadopentetate dimeglumine administration. A series of 16, 20-second, standard spin-echo images were obtained with no acceleration. Images were reconstructed by using keyhole data from a time of interest during gadopentetate dimeglumine uptake combined with reference data from before contrast agent injection or at the end of the image series, well after enhancement had been achieved. The images presented here have an acceleration factor of four. That is, only one-fourth as many k-space lines were used from each time of interest during uptake as were acquired for the reference image. However, because complete data sets were collected, the data allowed comparison of images with acceleration factors varying from one to 128, depending on how much borrowed data was used. For this spin-echo image series, a TR msec/TE msec of 150/15, 450-mm field of view (FOV), 10-mm section thickness, and 128 phase-encoding steps were used. Second, a kidney of a healthy, normal volunteer was studied, also during gadopentetate dimeglumine administration. The keyhole method was used to accelerate small-flip-angle, gradient-echo images by a factor of five, from 6- to 1.2-second acquisition time. These 1.2-second images were repeated with a 0.3-second delay between them, giving 1.5-second temporal resolution for contrast agent uptake. For this image series, the parameters were 21/3.2, 440-mm FOV, 12-mm section thickness, and 51 phase-encoding steps (except for the reference image, which had 256 phase-encoding steps). For presentation here, the FOV was cropped to 220 mm and then interpolated to 256 × 256 for display.

• RESULTS

From the complete data sets for the transplanted kidney, frames 4, 7, and 13—taken before, during, and after gadopentetate dimeglumine uptake, respectively—are shown in Figure 2. Figure 3 plots cortical and medullary signal intensity versus time. Complete data sets were used for both figures.

Frame 7 (Fig 2b), taken during uptake, was reconstructed by using zero-filling and pre- and postcontrast reference data, and the results are shown in Figures 4a–4c, respectively; 32 k-space lines were used, requiring 5 seconds of acquisition time.

The behavior of the signal intensity of kidney parenchyma averaged over a large ROI (Fig 5) is shown in the plots in Figure 6. These show mean signal intensities calculated for the precontrast, uptake, and postcontrast frames (frames 4, 7, and 13) with various fractions of data borrowed from pre- and postcontrast frames and by using zero-filling. Regardless of the source of borrowed data (or whether zero-filling was used) the mean signal inten-

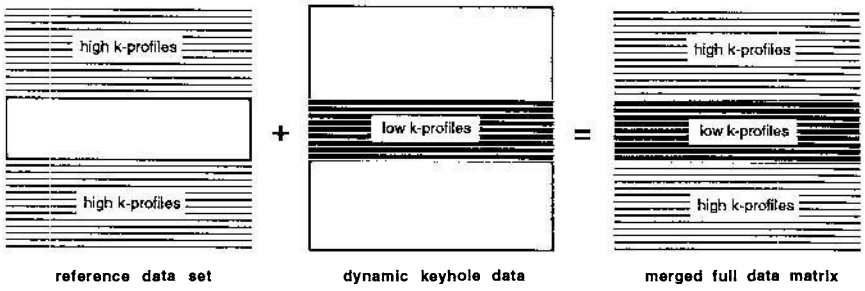

Figure 1. The high-frequency k-space profiles from a reference image acquired with a complete matrix (left) are merged with the low-frequency k-space profiles from a restricted keyhole of data (middle). Together they yield a complete data set (right) with the contrast of the dynamic keyhole data and the edge definition of the reference image.

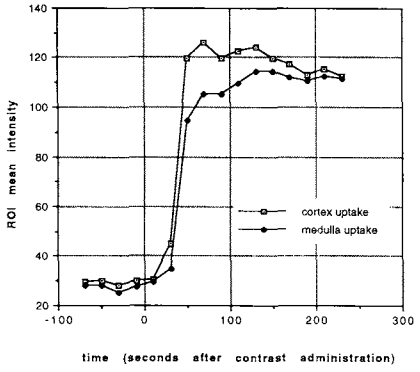

Figure 3. Plots of signal intensity versus time for kidney cortex and medulla computed in the regions of interest (ROIs) used in Figure 2.

Figure 2. Three frames from a 16-frame, dynamic series of images of a transplanted kidney: **(a)** precontrast image (frame 4), **(b)** image obtained during contrast agent uptake (frame 7), and **(c)** image obtained after contrast had stabilized. The same window settings were used for all images.

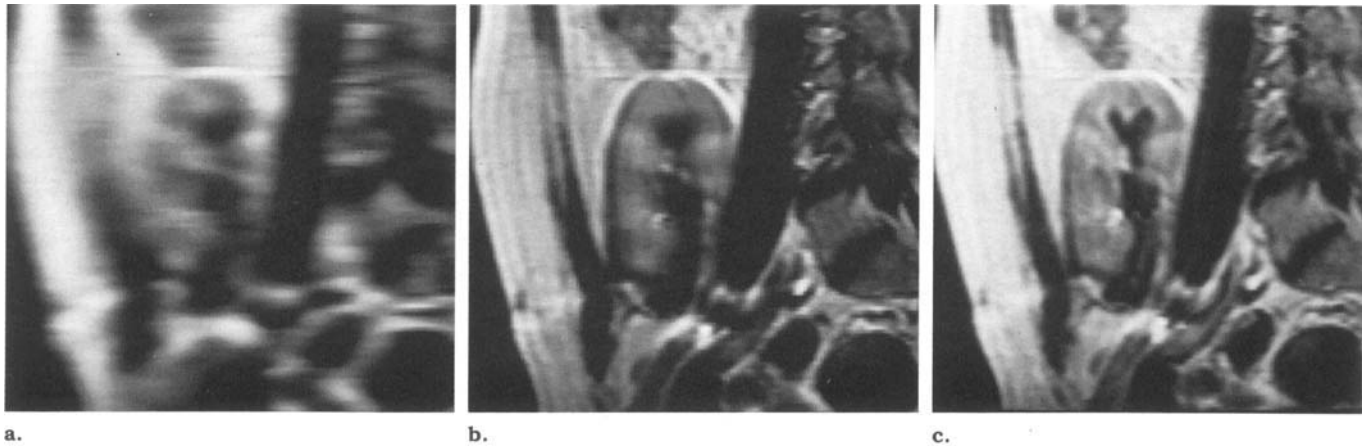

Figure 4. Keyhole and zero-filled reconstructions of frame 7 from the dynamic series of images of the transplanted kidney (Fig 2b). Each image used 32 lines of k space from frame 7; images **(a)** filled with 96 lines of zeros, **(b)** using 96 k-space lines averaged from precontrast frames 1–4, and **(c)** using lines averaged from postcontrast frames 12–15 are shown.

sities were stable for all borrowed data fractions up to 80%.

The plots in Figure 7 show the effect of borrowed data on signal intensity in four smaller ROIs (Fig 8) in the kidney medulla. Calculations were made for frame 7—obtained during uptake—with various fractions of zero-filling (Fig 7a) or borrowing of data from precontrast (Fig 7b) or postcontrast (Fig 7c) data sets. Similar calculations were made for four regions of cortex (not shown). In all ROIs tested, in both cortex and medulla, the signal intensities were stable with borrowed data fractions up to 60%.

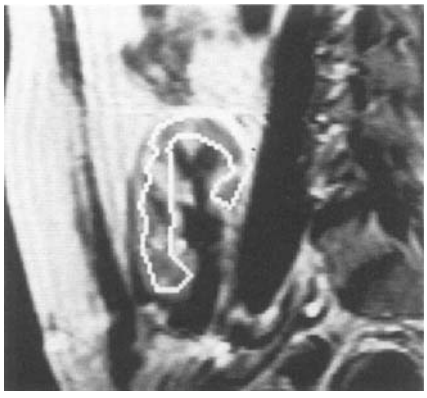

Figure 5. ROI for calculation of a single plot of contrast agent uptake in kidney parenchyma (both cortex and medulla).

Figures 2–8 are all based on the same dynamic series of images of a kidney transplant patient. The experiment with the normal volunteer, in which only 20% of each matrix was collected, is illustrated in Figures 9 and 10. Figure 9 shows the reference image obtained in 6 seconds. Figure 10 presents selected frames of the 64-frame series of keyhole images. Contrast changes are obvious 6–10.5 seconds after intravenous injection of gadopentetate dimeglumine. Progressive enhancement of the renal cortex is noted, accentuating corticomedullary distinction. The frame obtained 12 seconds after injection shows the kidneys at the most caudal position of a respiratory cycle, with the left kidney about half of a vertebral body height lower than on earlier frames. The 16.5-second frame shows the kidneys again in a more cranial position.

• DISCUSSION

The experiment using full data sets collected from the transplant patient shows the mathematical feasibility of the method and how large a speed increase can be expected. The volunteer experiment, with reduced data acquisitions, verifies that these expectations can actually be met despite respiratory motion (not a problem for transplanted kidneys) or unanticipated imager complications. Visually acceptable images were obtained with substantially reduced data collection times.

For the transplant patient, the zero-filled image (Fig 4a) is blurred as expected, while the keyhole images (Fig 4b, 4c) have edge definition similar to that of the standard, full-matrix image (Fig 2b). Contrast between the parenchyma and the calyces was much better with postcontrast than with precontrast reference data. This is because both tissues have low signal intensity on precontrast images (Fig 2a); therefore, precontrast data cannot be used to differentiate parenchyma from the calyces.

How far can one accelerate image acquisition without producing serious contrast errors? Since this may depend on the size of the ROI and the times during contrast agent uptake when the image and the reference data are taken, plots were obtained for different ROIs with data from different frames. While considering this, one should keep in mind the relevant types of voxels or pixels. Reference pixels

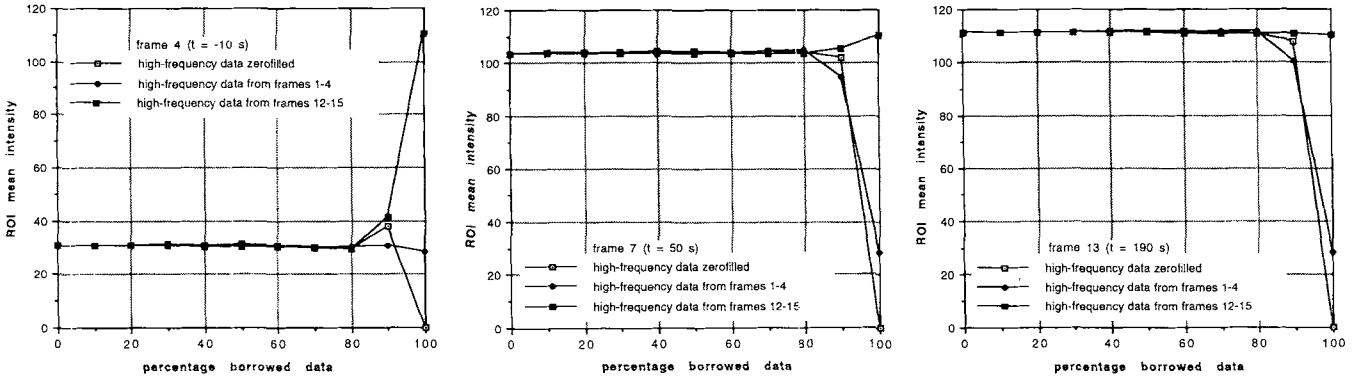

a. **b.** **c.**

Figure 6. Mean ROI signal intensity for kidney parenchyma (ROI in Fig 5) calculated with various percentages of borrowed data: **(a)** precontrast (frame 4), **(b)** during contrast agent uptake (frame 7), and **(c)** postcontrast (frame 13). Each set of plots shows results with high-frequency data zero-filled, borrowed from the average of frames 1–4, and borrowed from the average of frames 12–15.

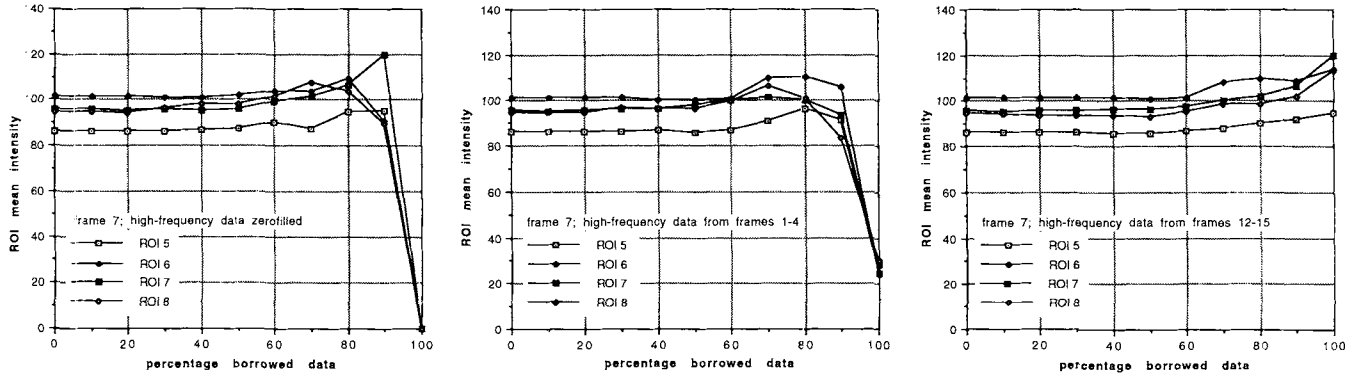

a. **b.** **c.**

Figure 7. Mean signal intensities for several kidney medullary ROIs (ROIs in Fig 8) during contrast agent uptake (frame 7) calculated with various percentages of borrowed data, with high-frequency data **(a)** zero-filled, **(b)** from precontrast frames 1–4, and **(c)** from postcontrast frames 12–15.

are determined by the acquisition of the reference images, while true, or keyhole, pixels are larger in the phase-encoding direction (but not in the other two directions) by the ratio of the number of phase-encoding steps used in the reference image to the number used in the repeated keyhole segments. This does not take into account any additional pixel interpolation for display purposes.

The largest ROI, used for whole-kidney signal intensity measurements (Figs 5, 6), avoids a region that is eight reference pixels wide in the phase-encoding direction at the margin of the kidney because this margin might be expected to contain the most severe ringing artifact when only one-fourth of the data are used (10). With this ROI, up to 80% of the data can be borrowed from a reference image (or zero-filled) without changing the measured signal intensity appreciably (Fig 6). This is true regardless of when the image and reference data are obtained.

Separate measurements of cortex and medulla require smaller ROIs and hence are more sensitive to contamination by signals from outside the ROIs if large acceleration factors are used. Figure 7 reveals no problems in medullary ROIs when up to 60% of the data is borrowed. This was also true for ROIs in the cortex. Figures 6 and 7 show that the signal intensities are stable up to a certain fraction of borrowed data; beyond that, as expected, the intensities tend toward the value of the source of the borrowed data (precontrast, postcontrast, or zero-filled), reaching that value when 100% of the data is borrowed.

The keyhole method combines the spatial detail of full-matrix images with the temporal resolution of a series of rapidly acquired, reduced-matrix images; however, it does not contain the same information as a series of rapidly acquired, full-matrix images, such as might result by using a shorter TR. What advantages does a series of keyhole images have over a series of zero-filled images in making a plot of signal intensity versus time such as in Figure 3?

The information contributed by new rows of data near the center of k space is exactly the same whether zero-filling or keyhole reconstruction is used. However, the better appearance of keyhole images results in two advantages over zero-filling in producing good signal-time plots. First, with anatomic knowledge of an area of interest, a high-resolution keyhole image allows accurate ROI placement so that inaccurate ROI placement does not compound the unavoidable inaccuracy caused by blurring. Conversely, when an interesting pattern of contrast agent uptake is observed, the keyhole method allows one to determine with greater certainty what is enhancing (eg, cortex or medulla). These same benefits are obtained in spectroscopic imaging by superimposing low-resolution images of rare metabolites on a standard proton image by using color (11). With the keyhole method, however, color equipment is not required.

In the experiment with the normal volunteer, problems were expected from res-

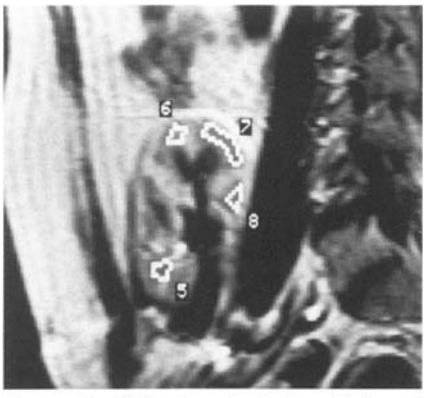

Figure 8. ROIs for calculation of plots of contrast agent uptake in medulla.

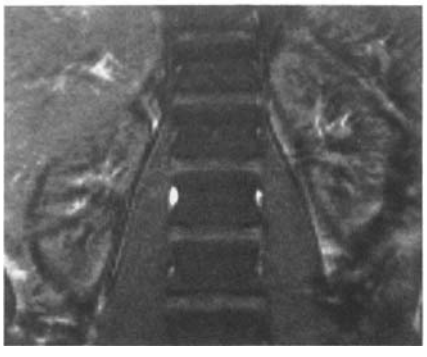

Figure 9. Gradient-echo reference image made with 256 rows in k space collected before contrast agent injection.

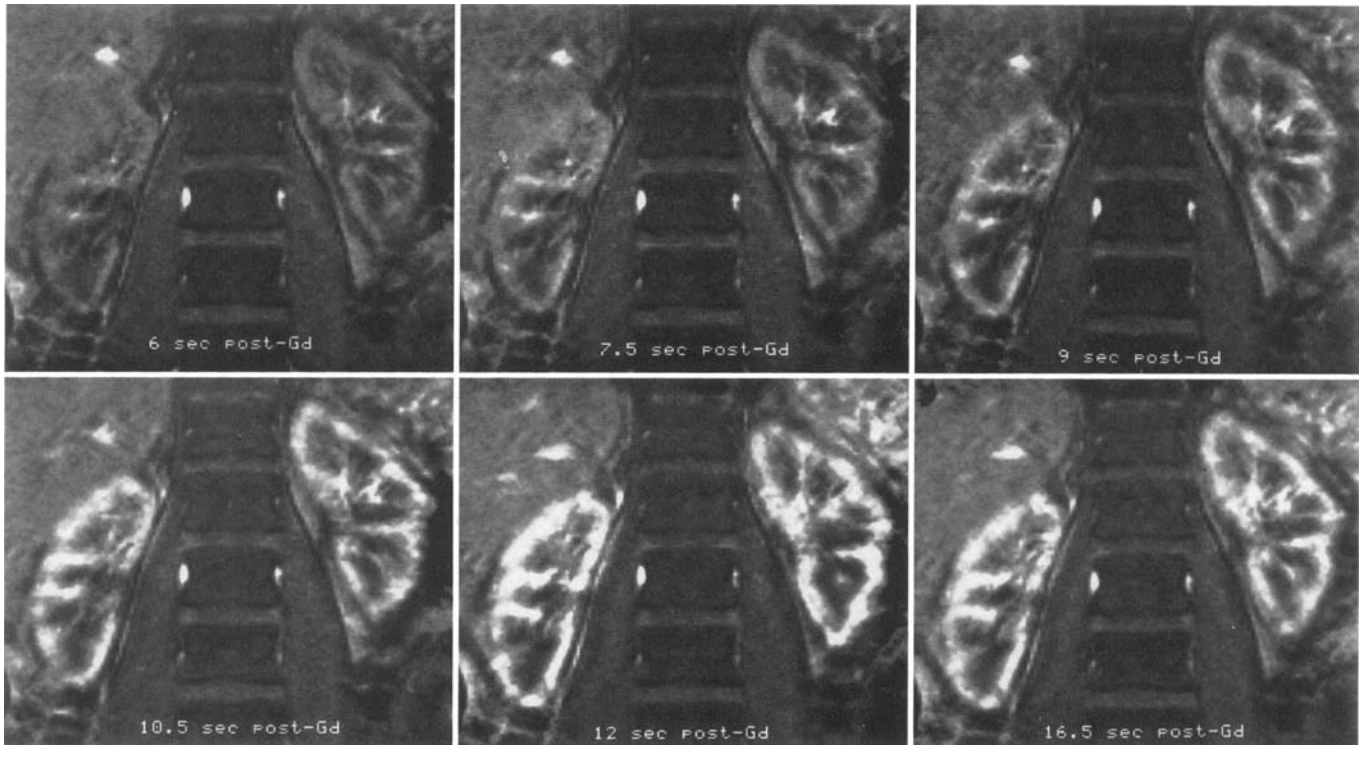

Figure 10. Dynamic keyhole images of gadopentetate dimeglumine uptake by the normal kidneys. Shown are six of 64 frames (obtained with the same settings) taken with 1.5-second resolution, as described in Materials and Methods. Reference data from Figure 9 were used. As the contrast agent bolus enters the kidneys, signal intensity in the cortex increases. Comparing the left kidney to the spine, especially in the 12-second frame, shows that the kidneys move with respiration, without substantially affecting edge sharpness.

piratory motion because much of the high-frequency data for each dynamic image comes from a single reference image. However, in the dynamic images reconstructed with the keyhole technique, the displacement of the kidney relative to its position on the reference image is clearly seen (Fig 10). This kidney displacement is in the read direction; the data truncated by the keyhole method largely determine edge definition in the phase-encoding direction. The cephalic portion of the left kidney is approximately half of a vertebral body height lower in the frame 12 seconds after injection than in the preceding frames. In a subsequent frame at 16.5 seconds after injection, the left kidney has returned to a higher position. Surprisingly, no additional blurring was seen when comparing the dynamic images with the reference image, although no breath holding, retrospective triggering, or postprocessing other than combining data sets was used. Until the effects of motion on keyhole imaging are understood, we advise caution.

We found that the keyhole method is a simple method of accelerating imaging. Using simple spin-echo and gradient-echo techniques, we had no need to modify data from either the reference image or the image of interest before or after Fourier transformation. Perhaps care is required with more complicated sequences (4,5). Our experiments were done without shielded gradients at 1.5 T, and we have no reason to expect field dependence in the applicability of the keyhole method. No triggering or presaturation was used to reduce respiration, cardiac motion, or blood pulsation effects.

In conclusion, the keyhole method substantially reduces the imaging time per dynamic image and can be applied whenever the same section is imaged repetitively to monitor a change in contrast. It could also be used to increase the number of sections imaged during the contrast change.

We find that the method is simple to apply with ordinary clinical equipment, at least for three- to fivefold speed gains with spin-echo or gradient-echo sequences, and we believe it is compatible with most other methods of increasing speed, including half-Fourier reconstruction.

We studied contrast agent uptake, but the keyhole method could also be used in evoked response experiments. Some potential clinical applications are perfusion of the brain, inflow and outflow in diseased or transplanted kidneys, uptake of gadopentetate dimeglumine in breast carcinoma, differential diagnosis of hepatic lesions, and imaging of cardiac infarction. ●

Acknowledgment: We thank Olaiya Humphrey for preparing the manuscript.

References

1. Mansfield P, Pykett IL. Biological and medical imaging by NMR. J Magn Reson 1978; 29:355–373.
2. Belliveau JW, Kennedy DN, McKinstry RC, et al. Functional mapping of the human visual cortex by magnetic resonance imaging. Science 1991; 254:716–718.
3. van Vaals JJ, Tuithof HH, Dixon WT. Increased time resolution in dynamic imaging (abstr). JMRI 1992; 2(P):44.
4. Liang ZP, Lauterbur PC. Improved temporal/spatial resolution in functional imaging through generalized series reconstruction (abstr). In: Works in progress supplement to annual meeting program. Chicago, Ill: Society for Magnetic Resonance Imaging, 1992; S15.
5. Bishop JE, Soutar I, Kucharczyk W, Plewes DB. Rapid sequential imaging with shared-echo fast spin-echo MR imaging (abstr). In: Works in progress supplement to annual meeting program. Chicago, Ill: Society for Magnetic Resonance Imaging, 1992; S22.
6. van Vaals JJ, Engels H, de Graaf RG, et al. Method for accelerated perfusion imaging (abstr). In: Book of abstracts: Society of Magnetic Resonance in Medicine 1992. Berkeley, Calif: Society of Magnetic Resonance in Medicine, 1992; 1139.
7. Brummer ME, Dixon WT, Gerety B, Tuithof HH. Composite k-space windows (keyhole techniques) to improve temporal resolution in a dynamic series of images following contrast administration (abstr). In: Book of abstracts: Society of Magnetic Resonance in Medicine 1992. Berkeley, Calif: Society of Magnetic Resonance in Medicine, 1992; 4236.
8. Liang ZP, Lauterbur PC. Efficient time-sequential imaging through generalized series modeling: a simulation analysis (abstr). In: Book of abstracts: Society of Magnetic Resonance in Medicine 1992. Berkeley, Calif: Society of Magnetic Resonance in Medicine, 1992; 4266.
9. Jones RA, Haraldseth O, Miller TB, Rinck PA, Unsgard G, Oksendal AN. Dynamic contrast enhanced, NMR perfusion imaging of regional cerebral ischemia in rats using k space substitution (abstr). In: Book of abstracts: Society of Magnetic Resonance in Medicine 1992. Berkeley, Calif: Society of Magnetic Resonance in Medicine, 1992; 1138.
10. Tretter SA. Introduction to discrete time signal processing. New York, NY: Wiley, 1976; 227–233.
11. Nelson SJ, Taylor JS, Vigneron DB, Murphy-Boesch J, Brown TR. Metabolite images of the human arm: changes in spatial and temporal distribution of high energy phosphates during exercise. NMR Biomed 1991; 4:268–273.